Heliyon 10 (2024) e39169

Contents lists available at ScienceDirect

Heliyon

journal homepage: www.cell.com/heliyon

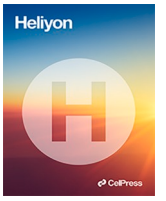

Research article

hsa_circ_0007755 competitively adsorbs miR-27b-3p to mediate CXCL2 expression and recruit Th1 cells to promote hypertrophic scars development

Jun Qi [a,*,1], YangYang Wu [a,1], YiFei Liu [b], JiuCheng Ma [c], ZhaoNan Wang [c]

[a] Department of Burn and Plastic Surgery, Affiliated Hospital of Nantong University, Nantong City, Jiangsu Province, 226001, China
[b] Department of Pathology, Affiliated Hospital of Nantong University, Nantong City, Jiangsu Province, 226001, China
[c] Nantong University, Nantong City, Jiangsu Province, 226001, China

ARTICLE INFO

Keywords:
Hypertrophic scars
circRNA
T-helper type 1 cells
Fibrogenesis
ceRNA pathway

ABSTRACT

Background and objective: The circular RNA hsa_circ_0007755 is markedly upregulated in hypertrophic scars (HS), yet its functional roles in this fibroproliferative disorder remain to be elucidated. This investigation aims to delineate the regulatory mechanisms of hsa_circ_0007755 in HS and to decode its downstream molecular signaling pathways.

Methods: We established a murine model of HS. Tissue histopathology was assessed using Hematoxylin and Eosin and Masson's trichrome staining. Peripheral blood from the animals was collected and the ratio of T-helper 1 (Th1) to T-helper 2 (Th2) cells was quantified via flow cytometry. The proliferation and apoptosis rates of human hypertrophic scar fibroblasts (hHSFs) were evaluated using the Cell Counting Kit-8 assay and flow cytometry, respectively. The invasive capacity of hHSFs was assessed via a Transwell assay. Co-culture experiments of hHSFs with T cells were conducted, and alterations in Th1/Th2 ratios were monitored using flow cytometry. Levels of cytokines, fibrosis-associated proteins, nuclear factor-kappaB (NF-κB) pathway-related protein, and C-X-C Motif Chemokine Ligand 2 (CXCL2) were quantified using Enzyme-Linked Immunosorbent Assay or Western blot analysis. The interactions between hsa_circ_0007755, miR-27b-3p, and CXCL2 were investigated using dual-luciferase reporter assays and RNA immunoprecipitation.

Results: Both hsa_circ_0007755 and CXCL2 were highly expressed in HS, whereas miR-27b-3p was downregulated. Knockdown of hsa_circ_0007755 inhibited the proliferation and invasion of hHSFs, promoted apoptosis, and reduced the expression of fibrotic proteins α-SMA and Collagen I, as well as the phosphorylation of the inflammatory pathway protein p65. Co-culture experiments confirmed that hHSFs lowly expressing hsa_circ_0007755 showed a decreased Th1 cell proportion and an increased Th2 cell proportion, alongside lower levels of TNF-α and INF-γ and higher levels of IL-4 and IL-10. The effects of either knocking down or overexpressing hsa_circ_0007755 were reversed by knocking down either miR-27b-3p or CXCL2, respectively. hsa_circ_0007755 acted as a "molecular sponge" for miR-27b-3p, sequestering and diminishing its availability, thereby alleviating its suppression of the target gene CXCL2.

* Corresponding author. Department of Burn and Plastic Surgery, Affiliated Hospital of Nantong University, No.20, Xisi Road, Chongchuan District, Nantong City, Jiangsu Province, 226001, China.
E-mail address: qijunsky@hotmail.com (J. Qi).
[1] Equal contributions to this study.

https://doi.org/10.1016/j.heliyon.2024.e39169
Received 28 December 2023; Received in revised form 8 October 2024; Accepted 8 October 2024
Available online 10 October 2024

Conclusion: hsa_circ_0007755 plays a pivotal role in modulating the immune response of HS by influencing the miR-27b-3p/CXCL2 axis, regulating the function and proportion of Th1 and Th2 cells, and thereby affecting the inflammatory and fibrotic processes in scar tissue.

1. Introduction

Hypertrophic scar (HS) is a fibrotic skin disease that usually occurs after wound healing and surgery [1]. In spite of many treatments available, there is no complete cure for HS. It is partly because of the complex immune responses that occur in HS, including the activation of T cells, particularly TH1 and TH2 [2–4]. T cells are the primary effector cells of cellular immunity, producing cytokines in the immune response and mediating inflammation [5]. Once the balance between TH1 cells and TH2 cells is disrupted, the malignant development of HS will be intensified [6]. In the immune system, TH1 cells and TH2 cells are considered key players, but their recruitment to the site of injury remains unclear.

circRNAs (circRNAs) are non-coding RNAs that can regulate miRNA activity and thus affect the expression of target genes [7–9]. It has been recently reported that circHECTD1 knockdown suppresses fibrosis in HS by interrupting transforming growth factor beta/Smad axis through miR-142-3p/high mobility group box-1 protein axis [10]. Moreover, circRNAs have recently been discussed to modulate immune responses. For example, differentially expressed circRNAs are correlated with TH1/TH2 differentiation pathways in radiation-induced lung injury [11]. In addition, circRNAs are involved in the TH1/TH2 immune response pathway in both cardiovascular disease and cancer [12,13]. As a result of these findings, it seems that circRNAs are important for regulating the immune response in HS, and that their role in controlling TH1/TH2 cells may be an effective target to combat or prevent this disease. A novel circRNA named hsa_circ_0007755 is abundantly expressed in HS [14,15]. However, it is not clear whether hsa_circ_0007755 is involved in regulating HS development.

This study investigated the role of hsa_cir_0007755 in immune response in HS. By regulating the miR-27b-3p/CXC motif chemokine ligand 2 (CXCL2) axis, hsa_cir_0007755 mediates TH1/TH2 balance, which may contribute to the fibrotic response in HS. This work highlights the potential of circRNA-mediated TH1/TH2 cell regulation as a therapeutic strategy to prevent or treat HS.

2. Materials and methods

2.1. Clinical samples

A cohort of 43 patients with HS, along with matched normal skin controls, was enrolled from Affiliated Hospital of Nantong University. Histopathological validation was performed on all tissue specimens. Specimens were cryogenically stored at −80 °C. Informed consent was duly obtained from all participants. The study protocol was approved by the Ethics Committee of Affiliated Hospital of Nantong University (Approval No: 20202NT116).

2.2. Quantitative real-time PCR (qRT-PCR)

Total RNA was extracted from cells and tissues using TRIzol reagent (Invitrogen, Carlsbad, CA, USA), and its integrity was assessed via a NanoDrop 2000 spectrophotometer. circRNA and mRNA were reverse transcribed into complementary DNA (cDNA) using the PrimeScript RT Master Mix Kit (Takara, RR036A, Japan). miRNA cDNA synthesis was conducted using the New Poly(A) Tailing Kit (Thermo Fisher, MA, USA). qRT-PCR was performed using the FastStart Universal SYBR Green Master (Roche, Mannheim, Germany)

Table 1
PCR sequences.

Genes	Sequences (5′–3′)
Human hsa_circ_0008667	Forward: 5′-CCCATTTCTAATACTGAAGGTGTCC-3′ Reverse: 5′-CTCCTCCTCAGAAGGTCCGA-3′
Mouse homologous hsa_circ_0008667	Forward: 5′-TCCAGTACTGAAGGTGTCCA -3′ Reverse: 5′-GGACCAGTCCAAAGCTACCC -3′
miR-370-3p	Forward: 5′-GCCTGCTGGGGTGGAA -3′ Reverse: 5′-TGGTGTCGTGGAGTCG-3′
Human VANGL1	Forward: 5′-CCTGAGTATCCAGCGAGCAG-3′ Reverse: 5′-ATGGAGGGGAAAATGGCCTG-3′
U6	Forward: 5′-CTCGCTTCGGCAGCACA-3′ Reverse: 5′-AACGCTTCACGAATTTGCGT-3′
Human GAPDH	Forward: 5′-GTCAAGGCTGAGAACGGGAA-3′ Reverse: 5′-AAATGAGCCCCAGCCTTCTC-3′
Mouse GAPDH	Forward: 5′-GGGTCCCAGCTTAGGTTCAT-3′ Reverse: 5′-GAAGGGGCGGAGATGATGAC-3′

Note: miR-370-3p, microRNA-370-3p; VANGL1, Van Gogh-like 1; GAPDH, glyceraldehyde-3-phosphate dehydrogenase.

and analyzed on an ABI PRISM 7900HT Sequence Detection System (Applied Biosystems, Waltham, MA, USA). U6 and Glyceraldehyde 3-phosphate dehydrogenase (GAPDH) served as internal reference genes, with primer sequences detailed in Table 1.

2.3. Cell culture

Human normal skin fibroblasts (HFF-1, SCRC-1041) and hyperplastic scar fibroblasts (hHSFs) were acquired from the American Type Culture Collection (ATCC). All cells were cultured in Dulbecco's Modified Eagle Medium (Gibco, Gaithersburg, MD, USA), supplemented with 10 % fetal bovine serum (FBS) (Gibco) and 1 % penicillin-streptomycin, in a controlled environment at 37 °C and 5 % CO2. All cells have been authenticated by STR profiling and tested negative for mycoplasma contamination.

2.4. Actinomycin D and RNase R treatment

The hHSFs were seeded in six-well plates at a density of 5×10^5 cells per well. Twenty-four hours post-seeding, the cells were exposed to 2 μg/mL actinomycin D (Sigma) and harvested at designated time points. RNA stability was analyzed using qRT-PCR. RNA from hHSFs (10 μg) was treated with RNase R (3 U/μg, Epicenter) and incubated at 37 °C for 30 min, followed by quantification of circRNA and linear RNA via qRT-PCR.

2.5. Cell transfection

Plasmids overexpressing hsa_circ_0007755 and CXCL2 and siRNAs, as well as miR-27b-3p mimics and inhibitors, were sourced from GenePharma (Shanghai, China). Transient transfection was performed using Lipofectamine® 2000 (Invitrogen; Thermo Fisher Scientific, Inc.) following the manufacturer's protocol. Forty-eight hours post-transfection, cells were harvested and the transfection efficiency was assessed by qRT-PCR or Western blot analysis.

2.6. Cell Counting Kit-8 (CCK-8)

Cell viability was assessed using the CCK-8 from Beyotime (Shanghai, China). Cells (5×10^3 cells/well) were seeded in a 96-well plate. At 0, 24, 48, and 72 h post-seeding, 10 μL of CCK-8 solution was added to each well, and the cells were incubated at 37 °C for 2 h. Absorbance at 450 nm was measured using a microplate reader (Thermo Fisher Scientific).

2.7. Flow cytometry

Cells were harvested and digested using trypsin. Apoptotic cells were detected using an apoptosis detection kit (Sigma-Aldrich Chemical Company, St Louis, MO, USA). Annexin-V-fluorescein isothiocyanate (FITC), propidium iodide (PI), and 4-(2-hydroxyethyl)-1-piperazineethanesulfonic acid buffer were combined in a ratio of 1:2:50 to formulate the Annexin-V-FITC/PI staining solution. Cells were resuspended in 100 μL of this staining solution at room temperature for 15 min, followed by the addition of 1 mL HEPES buffer. Apoptotic cells were quantified using a flow cytometer (BD Bioscience, USA) and data were analyzed using CellQuest software (Version 5.1; Becton-Dickinson and Company).

2.8. Transwell migration assay

Cell invasion was assessed using a Transwell apparatus separated by a polycarbonate membrane (8 μm pore size) coated with synthetic basement membrane. Cells (2×10^4) in serum-free medium were seeded into the upper chamber, while the lower chamber contained medium supplemented with 10 % FBS. After 24 h, cells on the upper surface were removed with a cotton swab, and cells that migrated to the lower surface were fixed and stained with crystal violet. Cells in three random fields were counted under a light microscope.

2.9. $CD4^+$ T cell isolation

$CD4^+$ T cells were purified from mouse lymph nodes and spleen using the Dynal® $CD4^+$ Negative Isolation Kit (Thermo Fisher Scientific) according to the manufacturer's instructions. Purified $CD4^+$ T cells were cultured in complete medium consisting of Roswell Park Memorial Institute 1640 supplemented with 10 % heat-inactivated FBS, 2 mM L-glutamine, 100 U/mL penicillin, and 100 μg/mL streptomycin. Purity of the isolated $CD4^+$ T cells was verified by flow cytometry.

2.10. Co-culture of $CD4^+$ T cells and hHSFs

$CD4^+$ T cells were seeded in 24-well plates at 1×10^5 cells per well and activated using anti-CD3 and anti-CD28 antibodies (BD Biosciences). Th1 cells were differentiated using 20 ng/mL interleukin (IL)-12 (R&D Systems, Minneapolis, MN, USA) and 2.5 μg/mL anti-IL-4 antibody (BD Biosciences), while Th2 cells were differentiated using 10 ng/mL IL-4 antibody, 250 U/mL IL-2, and 10 μg/mL interferon-gamma (INF-γ). After 4 days of differentiation, transfected or untransfected hHSFs were added to the 24-well plates containing Th cells for a 24-h co-culture at a ratio of 1:10. To assess cell surface markers, T cells were isolated, and their phenotype was

analyzed by flow cytometry [16]. Th1 cells were labeled with CD4 and CCR5 markers (BD Biosciences), while Th2 cells were labeled with CD4 and CCR4 markers (BD Biosciences).

3. Enzyme-Linked Immunosorbent Assay (ELISA)

Cellular cytokines including Tumor Necrosis Factor-alpha (TNF-α), INF-γ, IL-4, and IL-10 were quantified in the culture supernatants using ELISA kits (Cell Signaling Technology), adhering strictly to the manufacturer's protocols.

3.1. Western blot

Total proteins were extracted from tissues and cells utilizing radioimmunoprecipitation assay buffer (Beyotime), and concentrations were determined using the bicinchoninic acid protein assay kit. Following denaturation, proteins were treated with sodium dodecyl sulfate-polyacrylamide gel electrophoresis and subsequently transferred to polyvinylidene fluoride membranes. The membranes were then blocked with 5 % non-fat milk in Tris-buffered saline containing 0.1 % Tween 20 (TBST) and incubated at room temperature for 1 h. After blocking, the membranes were incubated with primary antibodies overnight at 4 °C. The membranes were washed thrice with TBST, each for 10 min, followed by incubation with horseradish peroxidase-conjugated secondary anti-rabbit immunoglobulin G (IgG) (heavy chain + light chain) (1:10,000, AB175781, Abcam) at room temperature for 1 h. After three subsequent TBST washes, chemiluminescent detection was performed, and images were acquired. Band intensity was quantified using ImagePro Plus 6.0 software. GAPDH served as the loading control. Primary antibodies used were: CXCL2 (MAB452, R&D Systems), Ki-67 (M7240, Dako), phospho-p65 (3033, Cell Signaling Technology), α-smooth muscle actin (α-SMA) (A5228, MilliporeSigma), collagen I (ab34710, Abcam), and GAPDH (ab8245, Abcam).

3.2. Dual-luciferase reporter assay

To elucidate the interactions between hsa_circ_0007755, CXCL2, and miR-27b-3p, sequences containing putative miR-27b-3p target sites were synthesized and cloned into the pMIR-REPORT™ vector (Thermo Fisher Scientific Inc.), resulting in constructs named wild-type hsa_circ_0007755 (WT-hsa_circ_0007755) and wild-type CXCL2 (WT-CXCL2). Mutant variants lacking the miR-27b-3p complementary sites (MUT-hsa_circ_0007755 and MUT-CXCL2) were also generated. These reporter vectors were co-transfected with mimic NC and miR-27b-3p mimic into HFF-1 cells. Forty-eight hours post-transfection, luciferase activity was measured using the Dual-Luciferase Reporter Assay System (Promega).

3.3. RNA immunoprecipitation (RIP) experiment

The Magna RIP RNA-Binding Protein Immunoprecipitation Kit (Millipore) was employed to isolate target RNA-protein complexes. Cells were lysed and suspended in RIP lysis buffer. RIP was performed using anti-Argonaute2 (Millipore) or normal mouse IgG (Millipore) as negative control, designated as Ago2 group and IgG group, respectively. Antibodies and protein A/G magnetic beads were incubated at 4 °C for 1 h. Target RNAs co-precipitated with the beads were then isolated and quantified by qRT-PCR.

3.4. Animal experiments

All animal experiments were approved by the Animal Care and Use Committee of Affiliated Hospital of Nantong University (Approval No: 20206NT127). Twenty-four male C57BL/6 mice (6–8 weeks, 18–25 g) were obtained from Hunan SJA Laboratory Animal Co., Ltd., and maintained under standard laboratory conditions with ad libitum access to food and water. To establish a HS animal model, sterile wounds of 1 cm in diameter were created bilaterally on the flanks of 18 mice, with a distance of 2 cm between adjacent wounds (bilateral symmetry). One week prior to surgery, adeno-associated virus short hairpin RNA targeting hsa_circ_0007755 (AAV-shRNA-hsa_circ_0007755) and control virus AAV-GFP-NC were injected intravenously (1.6×10^{11} vector genomes/mouse). Four weeks later, the mice were euthanized, blood samples were collected, and the TH1/TH2 ratio in blood was analyzed by flow cytometry [17]. Scar tissues were either fixed in 4 % paraformaldehyde or stored at −80 °C.

3.5. Histological staining (H&E)

Tissue samples were fixed in 4 % paraformaldehyde, dehydrated in graded ethanol, embedded in paraffin, and sectioned at 5 μm thickness. H&E and Masson's trichrome staining were employed to examine histological changes and collagen deposition [18].

3.6. Data analysis

Data presented as mean ± standard deviation (SD) were analyzed using SPSS software version 18.0. All experiments were performed with at least three biological replicates. Student's t-test was used for comparisons between two groups, and one-way analysis of variance was used for comparisons among three or more groups. A p-value <0.05 was considered statistically significant.

4. Results

4.1. hsa_circ_0007755 is abnormally highly expressed in HS

We initially characterized the expression profile of hsa_circ_0007755 in HS. As demonstrated in Fig. 1A–C, there was a pronounced upregulation of hsa_circ_0007755 in human HS tissues, murine HS models, and hHSFs, aligning with prior observations. Further analysis of its circular structure revealed that hsa_circ_0007755 was resistant to degradation by actinomycin D and RNase R, unlike linear mRNAs, confirming its identity as a novel circRNA highly expressed in HS contexts.

4.2. Silencing hsa_circ_0007755 inhibits proliferation, invasion, fibrosis, and inflammation of hHSFs

Following this, we introduced siRNAs targeting hsa_circ_0007755 into hHSFs. As depicted in Fig. 2A, si-hsa_circ_0007755 efficaciously reduced the expression levels of hsa_circ_0007755 in hHSFs. Cell proliferation assays, specifically CCK-8, demonstrated that downregulation of hsa_circ_0007755 reduced the proliferative abilities of hHSFs (Fig. 2B). Flow cytometric analysis indicated an elevation in apoptosis rates upon hsa_circ_0007755 knockdown (Fig. 2C). Transwell assays further showed a reduction in the invasive potential of hHSFs following hsa_circ_0007755 suppression (Fig. 2D). Western blot analysis confirmed the knockdown of hsa_circ_0007755 reduced the expression of proliferation marker Ki-67, fibrosis-associated proteins α-SMA and collagen I, and the inflammatory signaling protein p-p65 (Fig. 2E). To explore the effects of hsa_circ_0007755 on TH1/TH2 cell dynamics within HS, $CD4^+$ T cells were isolated and purified from murine lymph nodes and spleens (Fig. 2F). These cells were subsequently differentiated into TH1/TH2 cells and co-cultured with hsa_circ_0007755-silenced hHSFs. As shown in Fig. 2G, silencing hsa_circ_0007755 markedly decreased TH1 cell levels while increasing TH2 cell levels. Additionally, knockdown of hsa_circ_0007755 lowered the secretion of TH1 cytokines (TNF-α and INF-γ) and enhanced the release of TH2 cytokines (IL-4 and IL-10) (Fig. 2H). Collectively, these data suggest that silencing hsa_circ_0007755 can inhibit proliferation, invasion, and inflammation in hHSFs while promoting apoptosis.

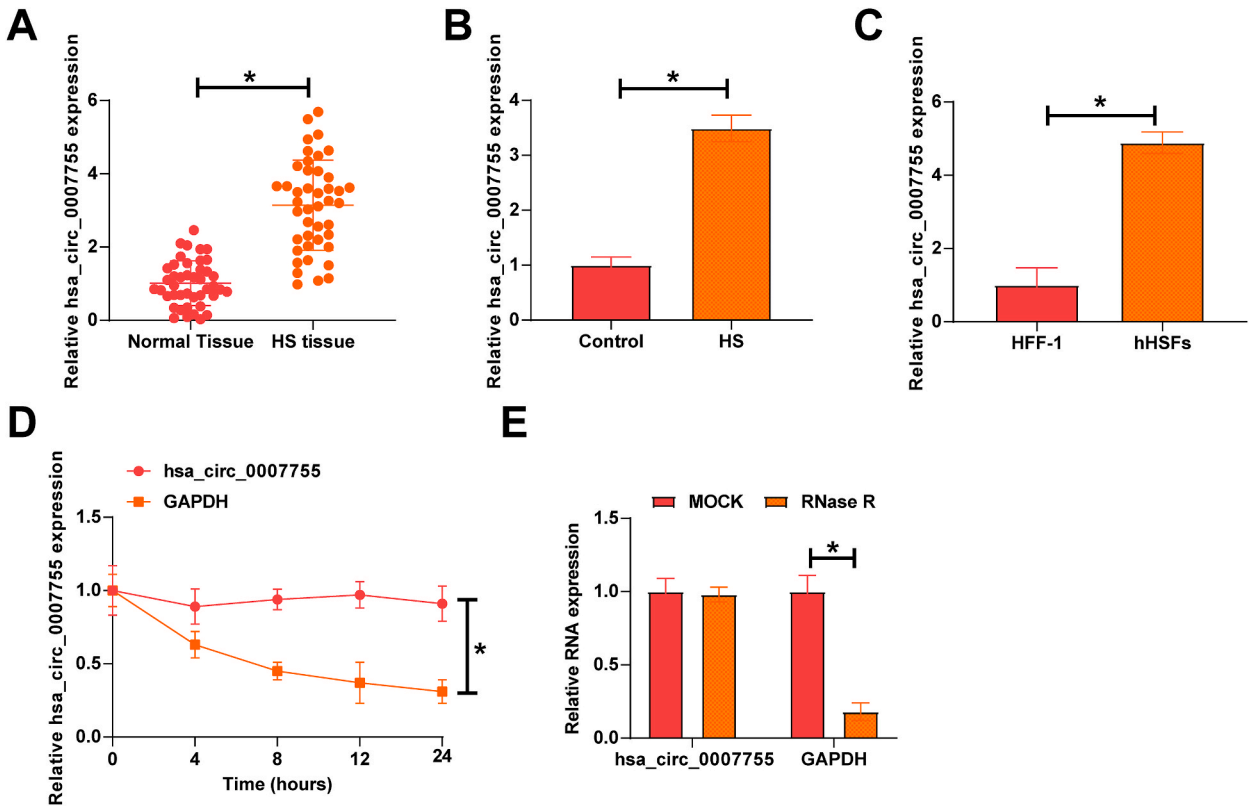

Fig. 1. hsa_circ_0007755 expression is high in HS.
A: qRT-PCR tested hsa_circ_0007755 in human normal skin tissue and HS tissue. B: qRT-PCR tested hsa_circ_0007755 in mouse normal skin tissue and HS tissue. C: qRT-PCR tested hsa_circ_0007755 in HFF-1 and hHSFs. D-F: Actinomycin D and RNAse R assayed the ring structure of hsa_circ_0007755. Data were expressed as mean ± SD (N = 3). $^*P < 0.05$.

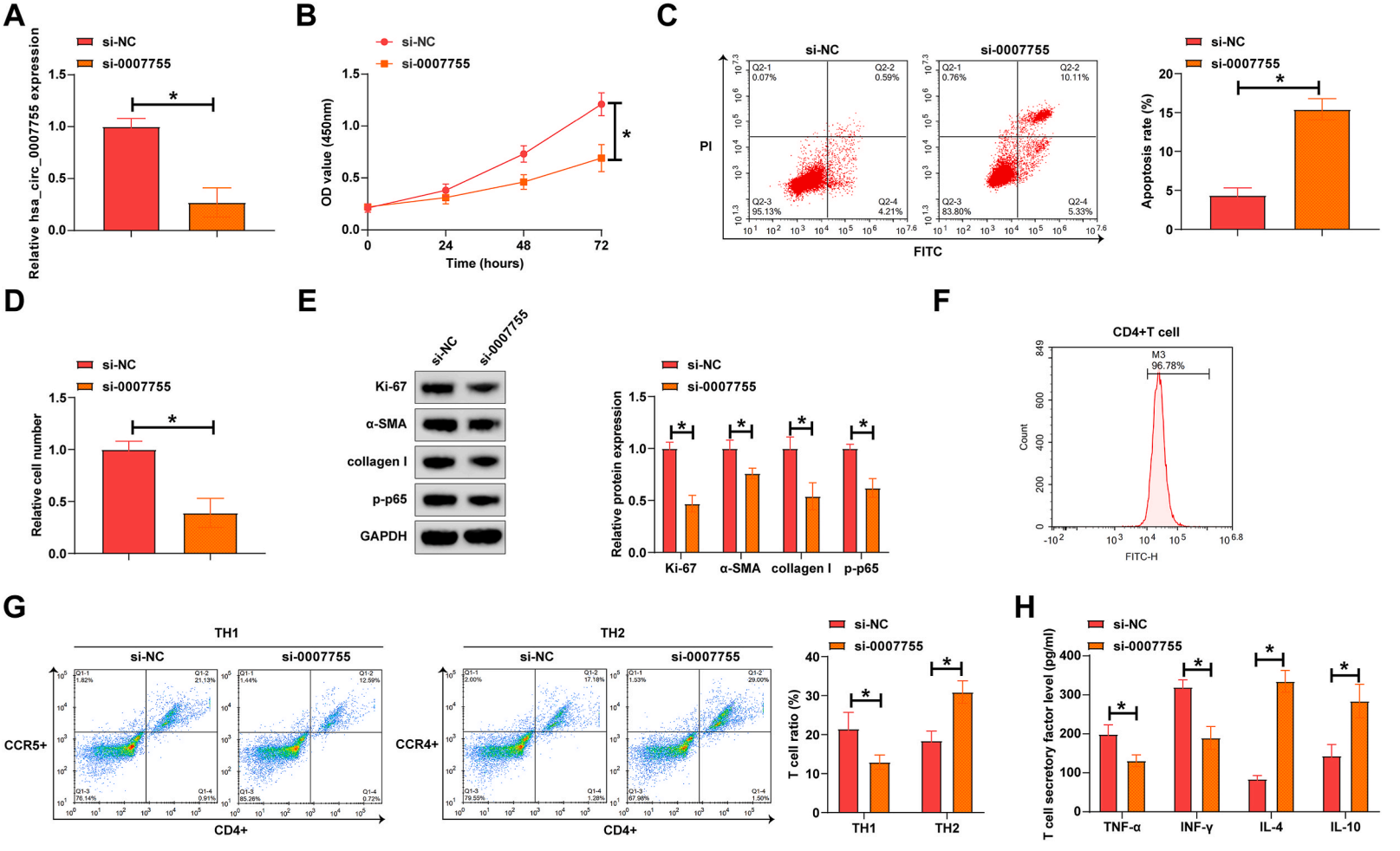

Fig. 2. Silencing hsa_circ_0007755 inhibits proliferation, invasion, fibrosis, and inflammation of hHSFs.
siRNA targeting hsa_circ_0007755 was transfected into hHSFs. A: qRT-PCR tested hsa_circ_0007755. B: CCK-8 assayed hHSFs proliferation. C: Flow cytometry measured apoptosis rate. D: Transwell assayed invasion ability. E: Western blot analyzed Ki-67, α-SMA, collagen I, and p-p65. F: Flow cytometry identified $CD4^{+}$T cells. G: Flow cytometry detection TH1/TH2 cell changes. H: ELISA measured cytokines TNF-α, INF-γ, IL-4, and IL-10 in TH1/TH2 cells. Data were expressed as mean ± SD (N = 3). *$P < 0.05$.

4.3. hsa_circ_0007755 targets mir-27b-3p

We next explored the downstream miRNAs interacting with hsa_circ_0007755. Bioinformatics tools identified a potential interaction site between hsa_circ_0007755 and miR-27b-3p (Fig. 3A). Subsequent qRT-PCR analysis revealed a marked downregulation of miR-27b-3p in human HS tissues, murine HS tissues, and hHSFs (Fig. 3B-D). To confirm the regulatory interaction between hsa_circ_0007755 and miR-27b-3p, dual-luciferase reporter assays and RIP experiments were conducted. As shown in Fig. 3E and F, co-transfection of WT-hsa_circ_0007755 and a miR-27b-3p mimic significantly reduced luciferase activity, with concurrent enrichment of both hsa_circ_0007755 and miR-27b-3p in Ago2-immunoprecipitated complexes. Moreover, silencing hsa_circ_0007755 resulted in increased miR-27b-3p expression in hHSFs (Fig. 3G). These findings confirm that hsa_circ_0007755 targets and modulates the expression of miR-27b-3p.

4.3.1. hsa_circ_0007755 plays a role in HS by regulating miR-27b-3p

Further investigations were conducted to determine whether miR-27b-3p participates in the regulatory mechanisms of HS mediated by hsa_circ_0007755. hHSFs were transfected either with miR-27b-3p mimic alone or co-transfected with pcDNA3.1-hsa_circ_0007755 and miR-27b-3p mimic. As depicted in Fig. 4A, miR-27b-3p mimic enhanced miR-27b-3p levels, whereas pcDNA3.1-hsa_circ_0007755 suppressed miR-27b-3p level; notably, miR-27b-3p mimic reversed the effects of pcDNA3.1-hsa_circ_0007755. CCK-8 assays revealed that overexpression of hsa_circ_0007755 accelerated the proliferation of hHSFs, an effect

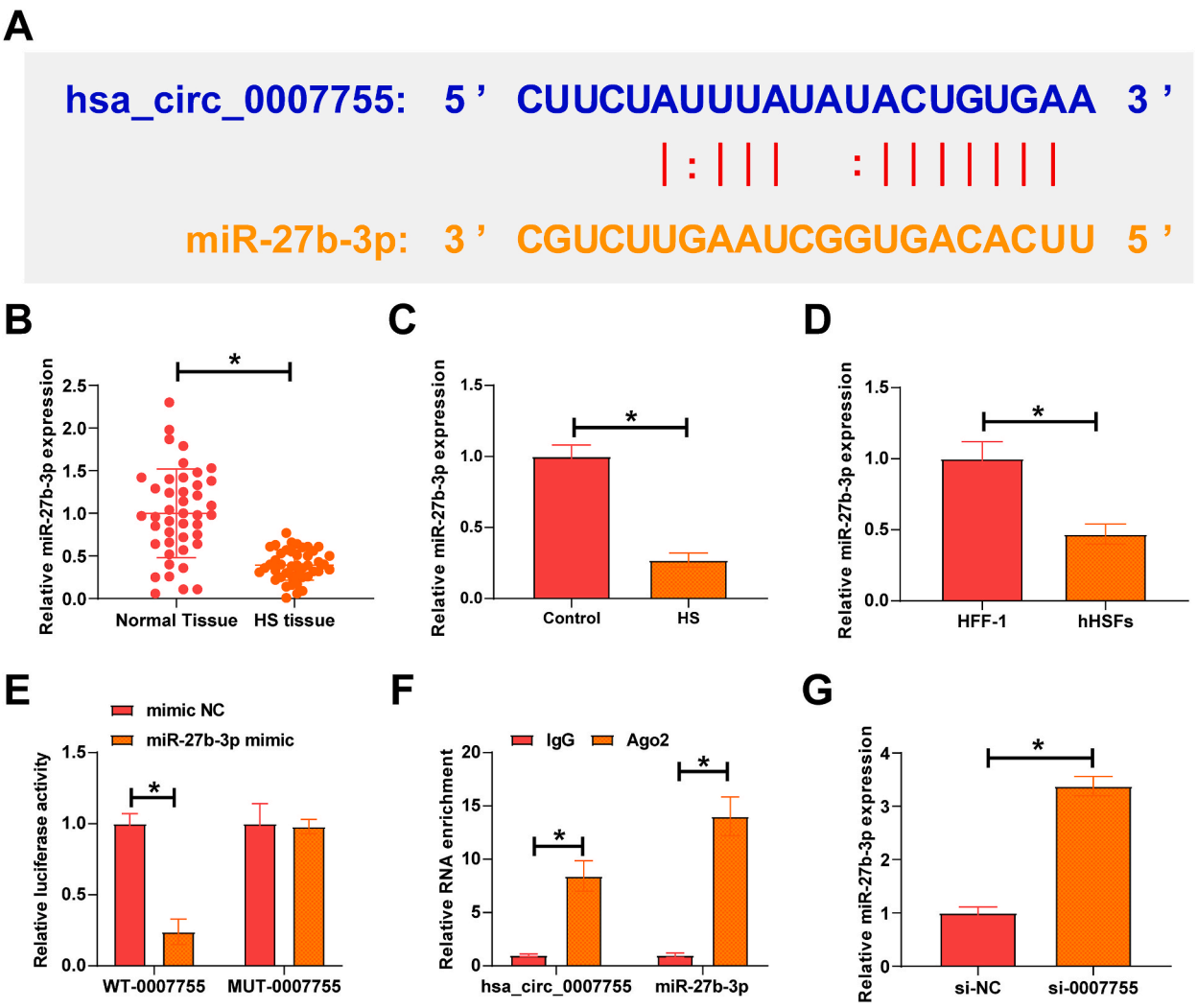

Fig. 3. hsa_circ_0007755 targets miR-27b-3p.
A: starbase predicted the potential binding sites of hsa_circ_0007755 and miR-27b-3p. B: qRT-PCR tested miR-27b-3p in human normal skin tissue and HS tissue. C: qRT-PCR tested miR-27b-3p in normal skin tissue and HS tissue of mice. D: qRT-PCR tested miR-27b-3p in HFF-1 and hHSFs. E-F: Dual luciferase reporter assay and RIP analyzed the targeting relationship between hsa_circ_0007755 and miR-27b-3p. G: qRT-PCR tested the effect of hsa_circ_0007755 knockdown on miR-27b-3p expression in hHSFs. Data were expressed as mean ± SD (N = 3). *$P < 0.05$.

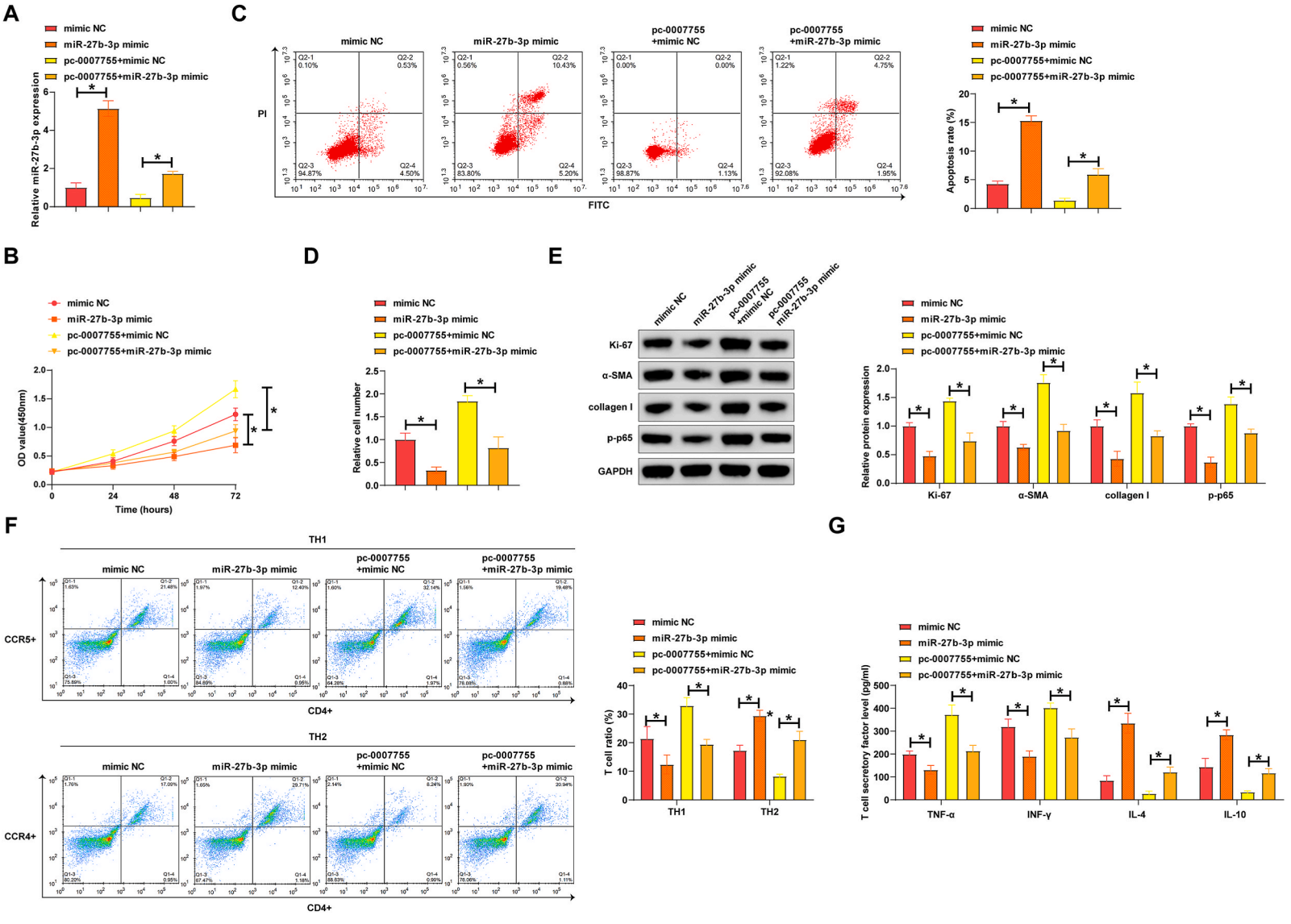

Fig. 4. hsa_circ_0007755 plays a role in HS by regulating miR-27b-3p.
miR-27b-3p mimic was transfected separately or pcDNA 3.1-hsa_circ_0007755 and miR-27b-3p mimic were co-transfected into hHSFs. A: qRT-PCR tested miR-27b-3p. B: CCK-8 assayed hHSF proliferation. C: Flow cytometry measured apoptosis rate. D: Transwell assayed invasion ability. E: Western blot analyzed Ki-67, α-SMA, collagen I, and p-p65. F: Flow cytometry detected TH1/TH2 cell changes. G: ELISA measured cytokines TNF-α, INF-γ, IL-4, and IL-10 in TH1/TH2 cells. Data were expressed as mean ± SD (N = 3). $^*P < 0.05$.

that was negated by overexpressing miR-27b-3p (Fig. 4B). Moreover, overexpression of hsa_circ_0007755 decreased apoptosis rates in hHSFs, while overexpression of miR-27b-3p increased apoptosis rates (Fig. 4C). Transwell assays confirmed that overexpressing hsa_circ_0007755 enhanced the invasive capabilities of the cells, which was reversed upon overexpressing miR-27b-3p (Fig. 4D). Overexpression of hsa_circ_0007755 upregulated the protein expressions of Ki-67, α-SMA, collagen I, and p-p65, whereas overexpressing miR-27b-3p inhibited these changes (Fig. 4E). Co-culture experiments demonstrated that overexpressing miR-27b-3p reduced TH1 cell levels, increased TH2 cell levels, decreased TNF-α and INF-γ levels, and elevated IL-4 and IL-10 levels; conversely, overexpressing hsa_circ_0007755 promoted TH1 differentiation and inhibited TH2 differentiation, effects that were reversible by overexpressing miR-27b-3p (Fig. 4F and G). These data elucidate that hsa_circ_0007755 modulates hHSF proliferation, invasion, apoptosis, and inflammation through the regulation of miR-27b-3p.

4.4. *A targeting relationship exists between mir-27b-3p and CXCL2*

We subsequently probed the downstream target genes of miR-27b-3p. Potential interaction sites between miR-27b-3p and CXCL2 were identified through the bioinformatics resource Starbase (Fig. 5A). Expression patterns of CXCL2 in HS were assessed via Western blot, revealing significant upregulation in human HS tissues, murine HS models, and hHSFs compared to normal controls (Fig. 5B-D). To ascertain the direct regulatory relationship between CXCL2 and miR-27b-3p, dual-luciferase reporter assays and RIP experiments were performed. Co-transfection of WT-CXCL2 and miR-27b-3p mimic significantly reduced luciferase activity, whereas co-transfection with MUT-CXCL2 and miR-27b-3p mimic did not affect luciferase activity (Fig. 5E and F). Additionally, a high enrichment of both CXCL2 and miR-27b-3p in Ago2 immunoprecipitates was observed. In functional gain-of-function experiments, overexpression of miR-27b-3p led to a decrease in CXCL2 protein levels (Fig. 5G). These findings confirm CXCL2 as a downstream target gene of miR-27b-3p.

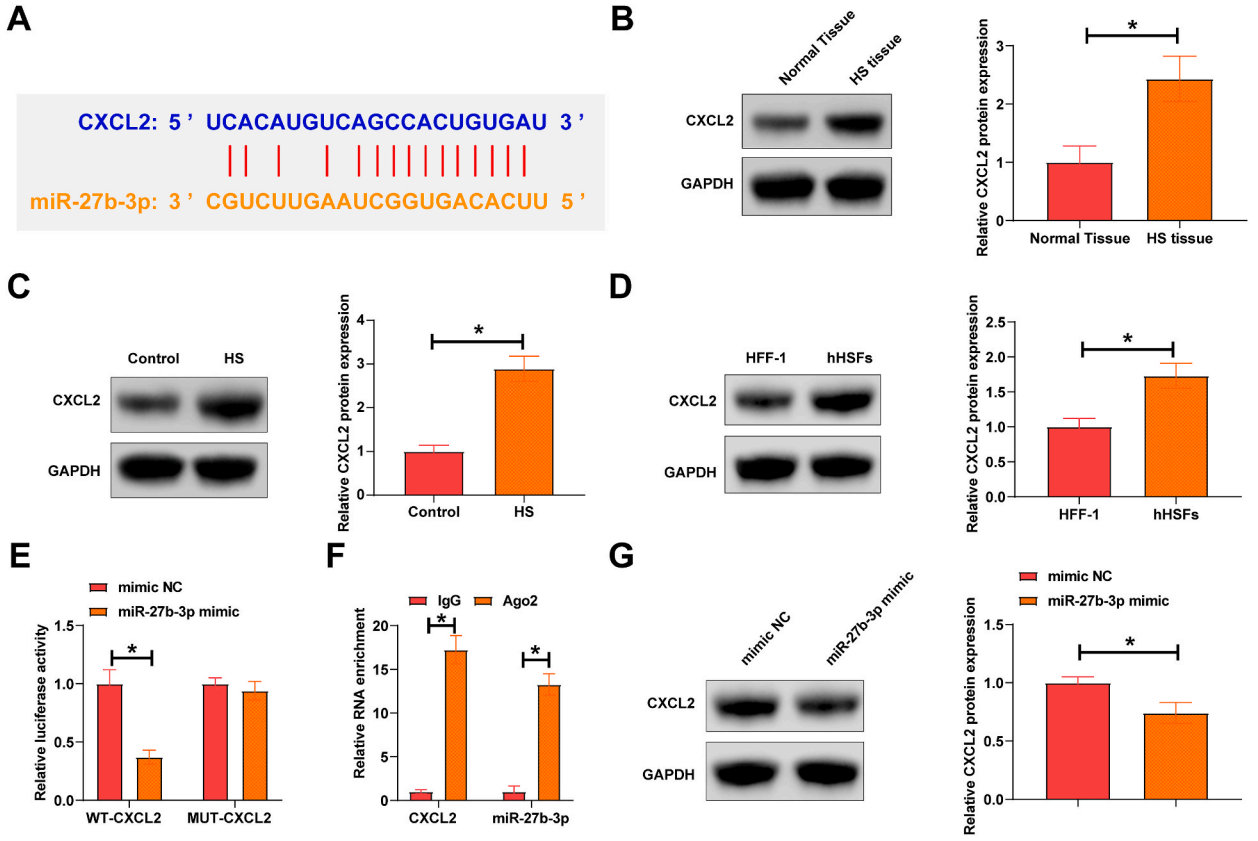

Fig. 5. CXCL2 is the target gene of miR-27b-3p.
A: starbase predicted the potential binding sites of CXCL2 and miR-27b-3p. B: Western blot tested CXCL2 in human normal skin tissue and HS tissue. C: Western blot tested CXCL2 in normal skin tissue and HS tissue of mice. D: Western blot tested CXCL2 in HFF-1 and hHSFs. E-F: Dual luciferase reporter assay and RIP analyzed the targeting relationship between CXCL2 and miR-27b-3p. G: Western blot tested the effect of overexpressed miR-27b-3p on CXCL2 expression in hHSFs. Data were expressed as mean ± SD (N = 3). *$P < 0.05$.

4.5. The promotion impact of hsa_circ_0007755 overexpression on proliferation, invasion, and inflammation of hHSFs is suppressed by knockdown of CXCL2

Subsequently, we co-transfected hHSFs with pcDNA3.1-hsa_circ_0007755 and siRNA targeting CXCL2. As shown in Fig. 6A, pcDNA3.1-hsa_circ_0007755 upregulated the expression of CXCL2, whereas si-CXCL2 led to a reduction in CXCL2 levels. CCK-8 proliferation assays demonstrated that hsa_circ_0007755 overexpression promoted the proliferative capacity of hHSFs, an effect counteracted by CXCL2 knockdown (Fig. 6B). Furthermore, overexpression of hsa_circ_0007755 decreased the apoptosis rate in hHSFs, an outcome reversed by silencing CXCL2 (Fig. 6C). Transwell invasion assays revealed that hsa_circ_0007755 overexpression enhanced cellular invasiveness, which was mitigated upon CXCL2 knockdown (Fig. 6D). Additionally, overexpression of hsa_circ_0007755 upregulated the protein expressions of Ki-67, α-SMA, collagen I, and p-p65, whereas CXCL2 knockdown prevented these protein alterations (Fig. 6E). Co-culture experiments indicated that hsa_circ_0007755 overexpression increased TH1 cell levels and decreased TH2 cell levels, effects that were reversed by CXCL2 knockdown (Fig. 6F). Moreover, hsa_circ_0007755 overexpression elevated the levels of TNF-α and INF-γ while reducing the levels of IL-4 and IL-10 (Fig. 6G). These data suggest that hsa_circ_0007755 mediates its effects in HS through the modulation of CXCL2.

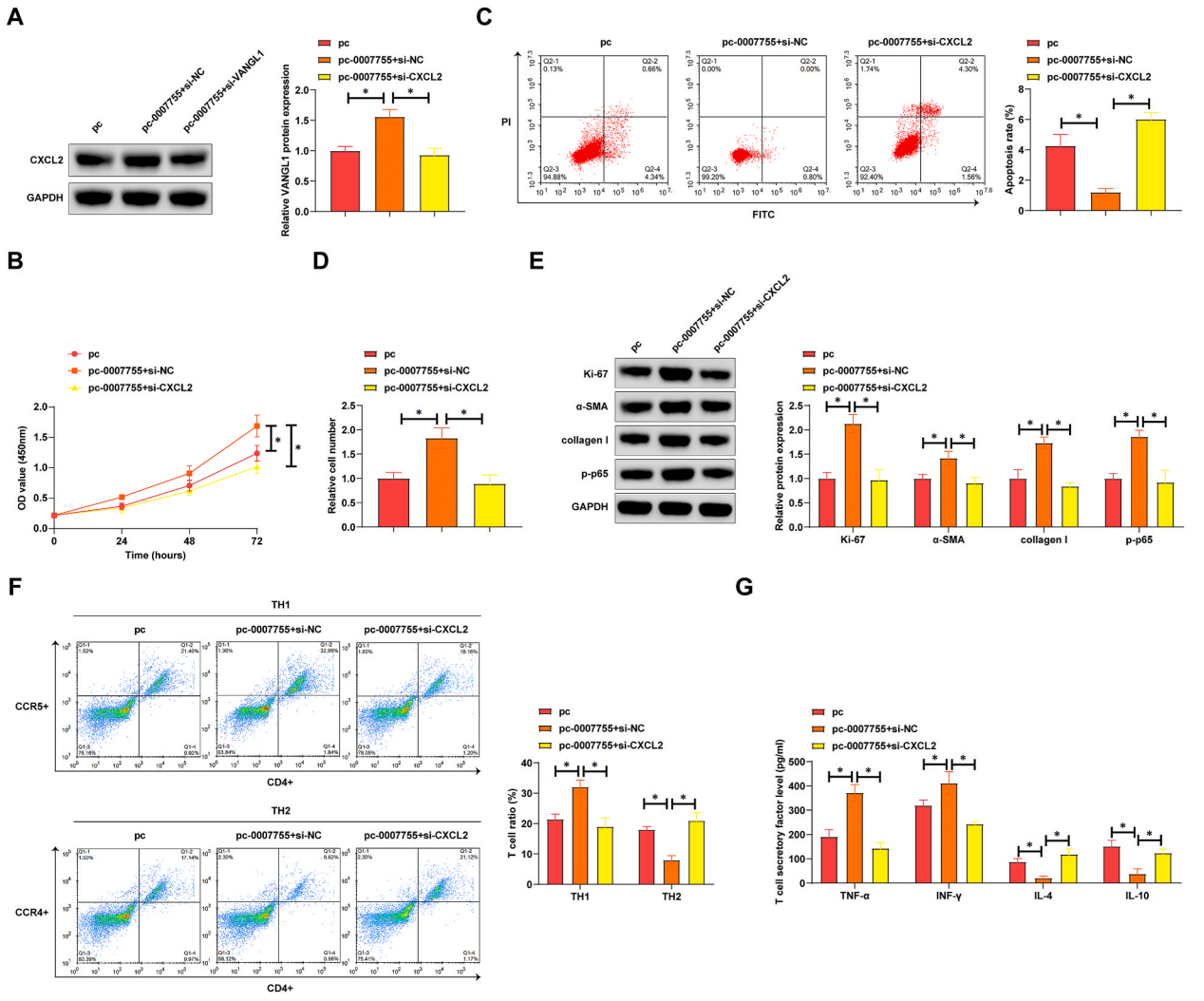

Fig. 6. The promotion effect of overexpressed hsa_circ_0007755 on proliferation, invasion and inflammation of hHSFs is mitigated by knockdown of CXCL2.

pcDNA 3.1-hsa_circ_0007755 and si-CXCL2 were co-transfected into hHSFs. A: Western blot tested CXCL2. B: CCK-8 assayed hHSFs proliferation. C: Flow cytometry measured apoptosis rate. D: Transwell assayed invasion ability. E: Western blot analyzed Ki-67, α-SMA, collagen I, and p-p65. F: Flow cytometry detected TH1/TH2 cell changes. G: ELISA measured cytokines TNF-α, INF-γ, IL-4, and IL-10 in TH1/TH2 cells. Data were expressed as mean ± SD (N = 3). *$P < 0.05$.

4.6. Low hsa_circ_0007755 inhibits HS and regulates TH1/TH2 balance in mice

Following this, we silenced hsa_circ_0007755 in HS mice model (Fig. 7A). Histological analysis using H&E and Masson's trichrome staining indicated that knockdown of hsa_circ_0007755 led to a reduction in scar formation and decreased fibrosis (Fig. 7B and C). Flow cytometric evaluation showed that silencing hsa_circ_0007755 decreased the proportion of TH1 cells and increased TH2 cells in murine blood (Fig. 7D). Moreover, this genetic modulation resulted in reduced serum levels of pro-inflammatory cytokines TNF-α and INF-γ and increased anti-inflammatory cytokines IL-4 and IL-10 (Fig. 7E). Western blot analysis confirmed the downregulation of CXCL2, Ki-67, α-SMA, collagen I, and p-p65 protein expression following hsa_circ_0007755 knockdown (Fig. 7F). These data suggest that *in vivo* silencing of hsa_circ_0007755 mitigates the development and progression of HS.

5. Discussion

There is a high degree of immune regulation involved in fibrosis in HS [19]. This study demonstrated that has_circ_0007755 mediates the miR-27b-3p/CXCL2 axis and is involved in HS immune response by affecting TH1/TH2 balance.

TH1 and TH2 cells are T helper cells, which are crucial for immune response [20]. TH1 cells produce pro-inflammatory cytokines to mediate cellular immunity, while TH2 cells produce anti-inflammatory cytokines to modulate humoral immunity [21,22]. Immune

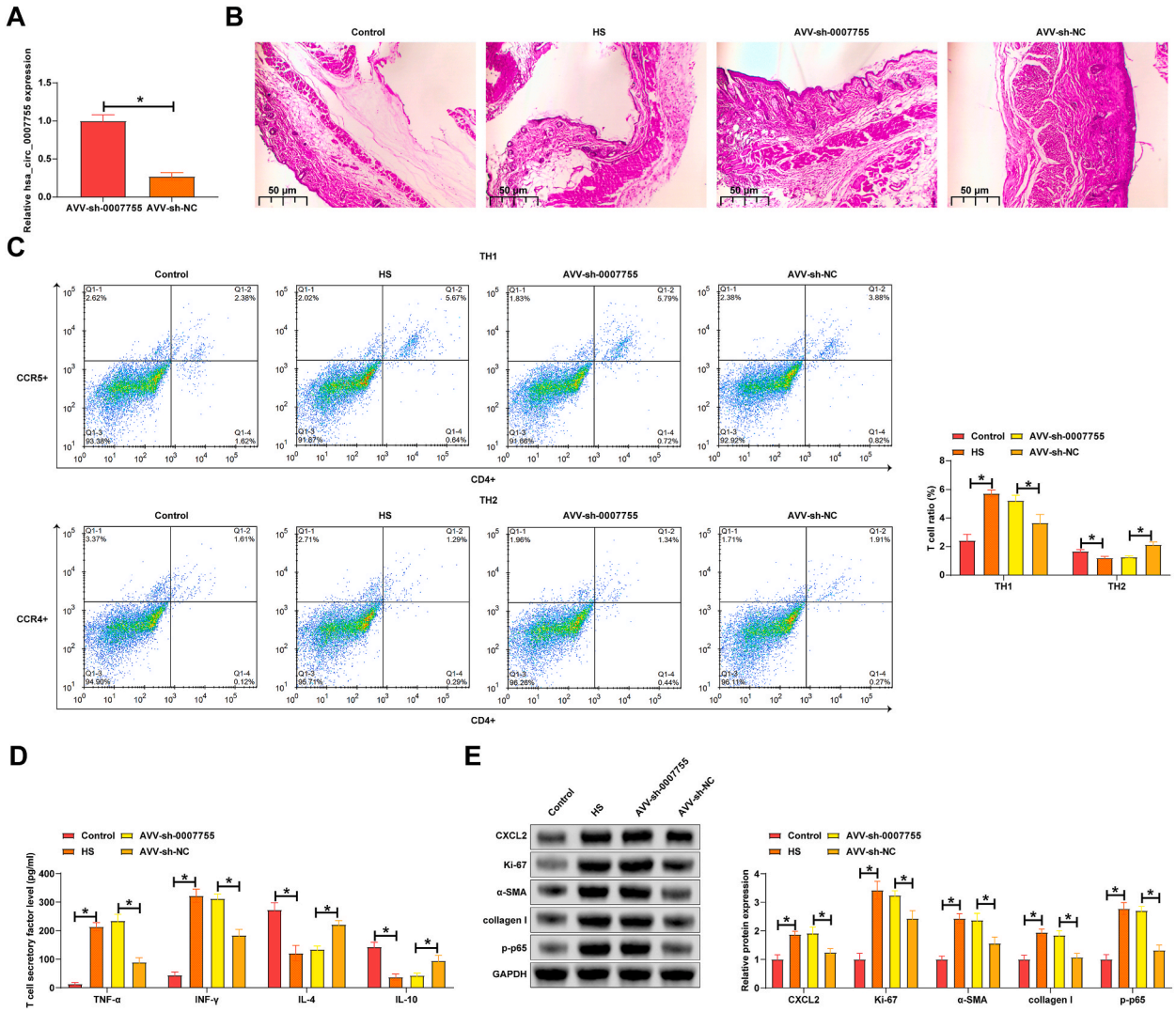

Fig. 7. Low hsa_circ_0007755 inhibits HS and regulates TH1/TH2 balance in mice.
A: Western blot tested hsa_circ_0007755. B: Representative images of HE staining of mouse scar tissue. C: Flow cytometry analyzed changes in TH1/TH2 ratio in mouse blood samples. D: ELISA measured serum levels of TNF-α, INF-γ, IL-4, and IL-10. E: Western blot tested CXCL2, Ki-67, α-SMA, collagen I, and p-p65 in mouse scar tissue. Data were expressed as mean ± SD (n = 6). *$P < 0.05$.

system function and health depend on balance between TH2 and TH1 cells [23–25]. Immune-mediated dermatosis may be mediated primarily by T cells, humoral immunity, or uncontrolled nonspecific inflammation [26–28], and an imbalance between TH1 and TH2 cells leads to chronic inflammation and fibrosis in HS [3]. This study noticed that hsa_cir_0007755 was highly expressed in human scar tissue. *In vitro* studies manifested that hsa_cir_0007755 knockdown reduced the proliferation and invasion of hHSF, enhanced apoptosis, and decreased fibrotic protein expression. These effects may be achieved by reducing TH1 cells and increasing TH2 cells.

One of the key pathways involved in the management of immune response is the NF-κB pathway, which regulates the activation and differentiation of immune cells [29–32]. In particular, activation of NF-κB affects TH1 and TH2 cell balance [33,34]. The study illustrated that overexpressing has_circ_0007755 promoted p-p65 expression and the release of inflammatory cytokines, contributing to TH1 cell increase and TH2 cell decrease.

CXCL2 is a chemokine that regulates immune response and fibrosis process [35,36]. A previous study highlights that CXCL2 is upregulated in HS and related to changes in TH1/TH2 balance in HS [3]. This study also had consistent results. hsa_cir_0007755 bound to miR-27b-3p to increase CXCL2 expression. CXCL2 is a key mediator in immune responses. By regulating miR-27b-3p and CXCL2, hsa_cir_0007755 can affect TH1 and TH2 cell balance, thereby affecting the overall immune response in HS. These findings have implications for understanding the underlying mechanisms of HS formation and for developing targeted treatment strategies for this condition.

Although this study explored the role of hsa_circ_0007755 using a mouse model and *in vitro* cultured hHSFs, these models inevitably limit the clinical applicability of the findings. First, there are significant immunological differences between mice and humans, particularly in the function and response of T cell subsets. Similarly, *in vitro* experiments have their limitations. While the hHSF culture system is effective in investigating the fundamental mechanisms of cell proliferation, apoptosis, and invasion, cellular behaviors *in vitro* often fail to accurately reflect the complex cell-cell and cell-microenvironment interactions occurring *in vivo*. Moreover, *in vitro* experiments cannot fully replicate the complete immune system and tissue microenvironment, which may overlook various signaling pathways and physiological effects involved when assessing the regulatory effects of hsa_circ_0007755 on Th1/Th2 cell balance and fibrosis. Given these limitations, future studies should prioritize more clinically relevant research, particularly validation using human samples. This approach would not only further confirm the role of hsa_circ_0007755 in hypertrophic scar formation but also provide stronger evidence for its feasibility as a potential therapeutic target.

This study preliminarily revealed the mechanism by which hsa_circ_0007755 acts as a "molecular sponge" to regulate miR-27b-3p and CXCL2, but this molecular network is likely more complex than currently understood. miR-27b-3p plays a broad role in various physiological and pathological processes [37,38], while CXCL2, as a chemokine, not only participates in immune cell recruitment but may also function in other pathological conditions [39,40]. Therefore, future studies should explore the broader interactions between hsa_circ_0007755, miR-27b-3p, and CXCL2, particularly whether additional, as-yet-undiscovered signaling pathways are involved. The dynamic changes in the immune system are highly intricate, and the Th1/Th2 cell ratio represents only part of the immune response. Other immune cell subsets, such as regulatory T cells [41] and natural killer cells [42], as well as various cytokine networks [43], also play crucial roles in scar formation. Future research should expand the scope of immune cell analysis to investigate the broader immunomodulatory effects of hsa_circ_0007755 on the entire immune system. To fully understand the role of hsa_circ_0007755 in HS, future studies should employ a variety of biological models for validation.

Together, the study highlights the critical role of hsa_cir_0007755 in regulating TH1 and TH2 cell balance in HS and provides new insights into the underlying mechanisms of this condition. Further studies are needed to fully understand the complex interactions between hsa_cir_0007755, miR-27b-3p, CXCL2, TH1, and TH2 cells and their effects on the immune response in HS. Moreover, the results apply only to mouse models and hHSFs cell models *in vitro*, and their applicability to humans is uncertain. A lot of groundwork needs to be done before clinical trials can proceed.

Availability of data and materials

The datasets used and/or analyzed during the present study are available from the corresponding author on reasonable request.

Ethics statement

The present study was approved by the Ethics Committee of Affiliated Hospital of Nantong University (No. 20202NT116) and written informed consent was provided by all patients prior to the study start. All procedures were performed in accordance with the ethical standards of the Institutional Review Board and The Declaration of Helsinki, and its later amendments or comparable ethical standards.

And the animal experiment research protocol was approved by Affiliated Hospital of Nantong University (No. 20206NT127) and performed in accordance with the “Guidelines for the care and use of experimental animals.”

CRediT authorship contribution statement

Jun Qi: Writing – review & editing, Writing – original draft, Supervision, Resources, Formal analysis, Conceptualization. **YangYang Wu:** Writing – original draft, Supervision, Resources, Investigation, Conceptualization. **YiFei Liu:** Methodology, Data curation. **JiuCheng Ma:** Investigation, Data curation. **ZhaoNan Wang:** Methodology, Formal analysis.

Funding

This study was supported by Nantong Burn Clinical Medical Research Center Project (HS2020006), Nantong Basic Science Research Project (JC2021181) and Nantong Municipal Guidance Project (MSZ2022085).

Declaration of competing interest

The authors declare that they have no known competing financial interests or personal relationships that could have appeared to influence the work reported in this paper.

Acknowledgments

Not applicable.

References

[1] J. Zhang, Y. Li, X. Bai, Y. Li, J. Shi, D. Hu, Recent advances in hypertrophic scar, Histol. Histopathol. 33 (1) (2018) 27–39.
[2] B. Chen, H. Li, W. Xia, Imiquimod regulating Th1 and Th2 cell-related chemokines to inhibit scar hyperplasia, Int. Wound J. 16 (6) (2019) 1281–1288.
[3] B. Chen, H. Li, W. Xia, The role of Th1/Th2 cell chemokine expression in hypertrophic scar, Int. Wound J. 17 (1) (2020) 197–205.
[4] V. Subramaniyan, S. Chakravarthi, R. Jegasothy, W.Y. Seng, N.K. Fuloria, S. Fuloria, et al., Alcohol-associated liver disease: a review on its pathophysiology, diagnosis and drug therapy, Toxicol Rep 8 (2021) 376–385.
[5] C. Dong, Cytokine regulation and function in T cells, Annu. Rev. Immunol. 39 (2021) 51–76.
[6] E.E. Tredget, L. Yang, M. Delehanty, H. Shankowsky, P.G. Scott, Polarized Th2 cytokine production in patients with hypertrophic scar following thermal injury, J. Interferon Cytokine Res. 26 (3) (2006) 179–189.
[7] L. Chen, C. Wang, H. Sun, J. Wang, Y. Liang, Y. Wang, et al., The bioinformatics toolbox for circRNA discovery and analysis, Brief Bioinform 22 (2) (2021) 1706–1728.
[8] J. Ju, Y.N. Song, X.Z. Chen, T. Wang, C.Y. Liu, K. Wang, circRNA is a potential target for cardiovascular diseases treatment, Mol. Cell. Biochem. 477 (2) (2022) 417–430.
[9] V. Kumarasamy, D. Anbazhagan, V. Subramaniyan, S. Vellasamy, Blastocystis sp., parasite associated with gastrointestinal disorders: an overview of its pathogenesis, immune modulation and therapeutic strategies, Curr Pharm Des 24 (27) (2018) 3172–3175.
[10] X. Ge, Y. Sun, Y. Tang, J. Lin, F. Zhou, G. Yao, et al., Circular RNA HECTD1 knockdown inhibits transforming growth factor-beta/small mothers against decapentaplegic (TGF-beta/Smad) signaling to reduce hypertrophic scar fibrosis, Bioengineered 13 (3) (2022) 7303–7315.
[11] Y. Li, L. Zou, L. Chu, L. Ye, J. Ni, X. Chu, et al., Identification and integrated analysis of circRNA and miRNA of radiation-induced lung injury in a mouse model, J. Inflamm. Res. 14 (2021) 4421–4431.
[12] P. Ginckels, P. Holvoet, Oxidative stress and inflammation in cardiovascular diseases and cancer: role of non-coding RNAs, Yale J. Biol. Med. 95 (1) (2022) 129–152.
[13] Collaborators GbdcoD, Global burden of 288 causes of death and life expectancy decomposition in 204 countries and territories and 811 subnational locations, 1990-2021: a systematic analysis for the Global Burden of Disease Study 2021, Lancet 403 (10440) (2024) 2100–2132.
[14] X. Li, Z. He, J. Zhang, Y. Han, Identification of crucial noncoding RNAs and mRNAs in hypertrophic scars via RNA sequencing, FEBS Open Bio 11 (6) (2021) 1673–1684.
[15] V. Subramaniyan, S. Fuloria, G. Gupta, D.H. Kumar, M. Sekar, K.V. Sathasivam, et al., A review on epidermal growth factor receptor's role in breast and non-small cell lung cancer, Chem. Biol. Interact. 351 (2022) 109735.
[16] P. Luz-Crawford, M. Kurte, J. Bravo-Alegria, R. Contreras, E. Nova-Lamperti, G. Tejedor, et al., Mesenchymal stem cells generate a CD4+CD25+Foxp3+ regulatory T cell population during the differentiation process of Th1 and Th17 cells, Stem Cell Res. Ther. 4 (3) (2013) 65.
[17] P. Huang, M. Zhou, S. Cheng, Y. Hu, M. Gao, Y. Ma, et al., Myricetin possesses anthelmintic activity and attenuates hepatic fibrosis via modulating TGFbeta1 and akt signaling and shifting Th1/Th2 balance in schistosoma japonicum-infected mice, Front. Immunol. 11 (2020) 593.
[18] Y. Li, J. Zhang, J. Shi, K. Liu, X. Wang, Y. Jia, et al., Exosomes derived from human adipose mesenchymal stem cells attenuate hypertrophic scar fibrosis by miR-192-5p/IL-17RA/Smad axis, Stem Cell Res. Ther. 12 (1) (2021) 221.
[19] Z.C. Wang, W.Y. Zhao, Y. Cao, Y.Q. Liu, Q. Sun, P. Shi, et al., The roles of inflammation in keloid and hypertrophic scars, Front. Immunol. 11 (2020) 603187.
[20] Y. Zhang, Y. Zhang, W. Gu, B. Sun, TH1/TH2 cell differentiation and molecular signals, Adv. Exp. Med. Biol. 841 (2014) 15–44.
[21] M.J. Butcher, J. Zhu, Recent advances in understanding the Th1/Th2 effector choice, Fac Rev 10 (2021) 30.
[22] V. Chinnasamy, V. Subramaniyan, S. Chandiran, S. Kayarohanam, D.C. Kanniyan, V. Velaga, et al., Antiarthritic activity of Achyranthes aspera on formaldehyde - induced arthritis in rats, Open Access Maced J Med Sci 7 (17) (2019) 2709–2714.
[23] Y. Bao, J. Peng, K.L. Yang, C.H. Wang, Y.F. Guo, Z.S. Guo, et al., Therapeutic effects of Chinese medicine Di-Long (Pheretima vulgaris) on rheumatoid arthritis through inhibiting NF-kappaB activation and regulating Th1/Th2 balance, Biomed. Pharmacother. 147 (2022) 112643.
[24] Z.G. Wang, G.Q. Shen, Y.H. Huang, Regulatory effects of miR-138 and RUNX3 on Th1/Th2 balance in peripheral blood of children with cough variant asthma, Zhong Guo Dang Dai Er Ke Za Zhi 23 (10) (2021) 1044–1049.
[25] L. Liu, S. Wang, H. Xing, Y. Sun, J. Ding, N. He, Bulleyaconitine A inhibits the lung inflammation and airway remodeling through restoring Th1/Th2 balance in asthmatic model mice, Biosci. Biotechnol. Biochem. 84 (7) (2020) 1409–1417.
[26] R. Sabat, K. Wolk, L. Loyal, W.D. Docke, K. Ghoreschi, T cell pathology in skin inflammation, Semin. Immunopathol. 41 (3) (2019) 359–377.
[27] A.W. Ho, T.S. Kupper, T cells and the skin: from protective immunity to inflammatory skin disorders, Nat. Rev. Immunol. 19 (8) (2019) 490–502.
[28] A.A. Bhat, O. Afzal, M. Afzal, G. Gupta, R. Thapa, H. Ali, et al., MALAT1: a key regulator in lung cancer pathogenesis and therapeutic targeting, Pathol. Res. Pract. 253 (2024) 154991.
[29] J. Dong, O. Xu, J. Wang, C. Shan, X. Ren, Luteolin ameliorates inflammation and Th1/Th2 imbalance via regulating the TLR4/NF-kappaB pathway in allergic rhinitis rats, Immunopharmacol. Immunotoxicol. 43 (3) (2021) 319–327.
[30] S.C. Sun, The non-canonical NF-kappaB pathway in immunity and inflammation, Nat. Rev. Immunol. 17 (9) (2017) 545–558.
[31] L. Barnabei, E. Laplantine, W. Mbongo, F. Rieux-Laucat, R. Weil, NF-kappaB: at the borders of autoimmunity and inflammation, Front. Immunol. 12 (2021) 716469.
[32] N. Sharma, I. Zahoor, M. Sachdeva, V. Subramaniyan, S. Fuloria, N.K. Fuloria, et al., Deciphering the role of nanoparticles for management of bacterial meningitis: an update on recent studies, Environ. Sci. Pollut. Res. Int. 28 (43) (2021) 60459–60476.
[33] X. Chen, M. Bi, J. Yang, J. Cai, H. Zhang, Y. Zhu, et al., Cadmium exposure triggers oxidative stress, necroptosis, Th1/Th2 imbalance and promotes inflammation through the TNF-alpha/NF-kappaB pathway in swine small intestine, J. Hazard Mater. 421 (2022) 126704.
[34] X. Bing, L. Xuelei, D. Wanwei, L. Linlang, C. Keyan, EGCG maintains Th1/Th2 balance and mitigates ulcerative colitis induced by dextran sulfate sodium through TLR4/MyD88/NF-kappaB signaling pathway in rats, Can J Gastroenterol Hepatol 2017 (2017) 3057268.

[35] A. Wree, M.D. McGeough, M.E. Inzaugarat, A. Eguchi, S. Schuster, C.D. Johnson, et al., NLRP3 inflammasome driven liver injury and fibrosis: roles of IL-17 and TNF in mice, Hepatology 67 (2) (2018) 736–749.
[36] G. De Rubis, K.R. Paudel, V. Allam, V. Malyla, V. Subramaniyan, S.K. Singh, et al., Involvement of osteopontin, EpCAM, estrogen receptor-alpha, and carbonic anhydrase IX protein in managing lung cancer via Berberine-loaded liquid crystalline nanoparticles, Pathol. Res. Pract. 253 (2024) 154971.
[37] Y. Tang, L.J. Yang, H. Liu, Y.J. Song, Q.Q. Yang, Y. Liu, et al., Exosomal miR-27b-3p secreted by visceral adipocytes contributes to endothelial inflammation and atherogenesis, Cell Rep. 42 (1) (2023) 111948.
[38] H. Zheng, J. Huang, M. Zhang, H.J. Zhao, P. Chen, Z.H. Zeng, miR-27b-3p improved high glucose-induced spermatogenic cell damage via regulating Gfpt1/HBP signaling, Eur. Surg. Res. 63 (2) (2022) 64–76.
[39] K. De Filippo, A. Dudeck, M. Hasenberg, E. Nye, N. van Rooijen, K. Hartmann, et al., Mast cell and macrophage chemokines CXCL1/CXCL2 control the early stage of neutrophil recruitment during tissue inflammation, Blood 121 (24) (2013) 4930–4937.
[40] W. Lin, Q. Li, L. Liu, Q. Wang, D. Zhang, F. Wang, et al., Early infiltrating NKT lymphocytes attenuate bone regeneration through secretion of CXCL2, Sci. Adv. 10 (20) (2024) eadl6343.
[41] J. Wu, B. Ren, D. Wang, H. Lin, Regulatory T cells in skeletal muscle repair and regeneration: recent insights, Cell Death Dis. 13 (8) (2022) 680.
[42] V.H. Hu, P.J. Luthert, T. Derrick, J. Pullin, H.A. Weiss, P. Massae, et al., Immunohistochemical analysis of scarring trachoma indicates infiltration by natural killer and undefined CD45 negative cells, PLoS Negl Trop Dis 10 (5) (2016) e0004734.
[43] J.K. Nguyen, E. Austin, A. Huang, A. Mamalis, J. Jagdeo, The IL-4/IL-13 axis in skin fibrosis and scarring: mechanistic concepts and therapeutic targets, Arch. Dermatol. Res. 312 (2) (2020) 81–92.